Local gene therapy durably restores vestibular function in a mouse model of Usher syndrome type 1G

Alice Emptoz, Vincent Michel, Andrea Lelli, Omar Akil, Jacques Boutet de Monvel, Ghizlene Lahlou, Anaïs Meyer, Typhaine Dupont, Sylvie Nouaille, Elody Ey, et al.

Local gene therapy durably restores vestibular function in a mouse model of Usher syndrome type 1G

Alice Emptoz[a,b,c], Vincent Michel[a,b,c], Andrea Lelli[a,b,c], Omar Akil[d], Jacques Boutet de Monvel[a,b,c], Ghizlene Lahlou[a,b,c], Anaïs Meyer[a,b], Typhaine Dupont[a,b,c], Sylvie Nouaille[a,b,c], Elody Ey[e], Filipa Franca de Barros[f], Mathieu Beraneck[f], Didier Dulon[g], Jean-Pierre Hardelin[a,b,c], Lawrence Lustig[h], Paul Avan[i], Christine Petit[a,b,c,j,1,2], and Saaid Safieddine[a,b,c,1,2]

[a]INSERM, UMR 1120, Paris, France; [b]Génétique et Physiologie de l'Audition, Institut Pasteur, 75015 Paris, France; [c]Complexité du Vivant, Sorbonne Universités, Université Pierre-et-Marie-Curie, Université Paris VI, 75015 Paris, France; [d]Otolaryngology-Head & Neck Surgery, University of California, San Francisco, CA 94117; [e]Unité de Génétique Humaine et Fonctions Cognitives, Institut Pasteur, CNRS UMR 3571, 75015 Paris, France; [f]Centre de Neurophysique, Physiologie, et Pathologie, CNRS UMR 8119, Université Paris-Descartes, 75006 Paris, France; [g]Laboratoire de Neurophysiologie de la Synapse Auditive, Bordeaux Neurocampus, INSERM, UMR 1120, Université de Bordeaux, 33076 Bordeaux, France; [h]Columbia University School of Medicine and New York Presbyterian Hospital, New York, NY 10034; [i]Laboratoire de Biophysique Sensorielle, Faculté de Médecine, Université d'Auvergne, Biophysique Médicale, Centre Jean Perrin, 63000 Clermont-Ferrand, France; and [j]Collège de France, 75005 Paris, France

Contributed by Christine Petit, July 27, 2017 (sent for review June 26, 2017; reviewed by Karen B. Avraham and Deniz Dalkara)

Our understanding of the mechanisms underlying inherited forms of inner ear deficits has considerably improved during the past 20 y, but we are still far from curative treatments. We investigated gene replacement as a strategy for restoring inner ear functions in a mouse model of Usher syndrome type 1G, characterized by congenital profound deafness and balance disorders. These mice lack the scaffold protein sans, which is involved both in the morphogenesis of the stereociliary bundle, the sensory antenna of inner ear hair cells, and in the mechanoelectrical transduction process. We show that a single delivery of the sans cDNA by the adenoassociated virus 8 to the inner ear of newborn mutant mice reestablishes the expression and targeting of the protein to the tips of stereocilia. The therapeutic gene restores the architecture and mechanosensitivity of stereociliary bundles, improves hearing thresholds, and durably rescues these mice from the balance defects. Our results open up new perspectives for efficient gene therapy of cochlear and vestibular disorders by showing that even severe dysmorphogenesis of stereociliary bundles can be corrected.

gene | therapy | balance | mouse | Usher

Patients affected by both sensorineuronal hearing impairment and balance disorders due to inner ear defects are currently fitted with auditory prostheses (hearing aids or cochlear implants) and can benefit from balance rehabilitation therapy, but the outcomes are different from one patient to another. Some individuals with congenital profound deafness are able to have phone conversations thanks to cochlear implants, whereas others obtain little or no benefit from these devices, beyond becoming aware of environmental sounds (1, 2). Such variability has been reported in patients with Usher syndrome type 1 (USH1) (Online Mendelian Inheritance in Man no. 276900) (3, 4). Patients with USH1 suffer from congenital profound deafness and balance defects, and they subsequently undergo sight loss leading to blindness. The loss of visual input impedes lip reading and greatly limits vestibular defect compensation.

We tested local gene replacement as an alternative approach to cure deafness and balance disorders of USH1. The anatomy of the human inner ear is suitable for gene therapy. Its relatively isolated fluid-filled compartments allow one to deliver recombinant viral particles locally while minimizing the risk of systemic dissemination. The inner ear contains the hearing organ (the cochlea) and five vestibular end organs devoted to equilibration (the utricle and saccule, which detect linear acceleration, and three semicircular canals, each housing an ampulla, which detect angular accelerations of head rotation) (Fig. 1*A*). Sound and acceleration are detected by the mechanosensory receptor cells (hair cells) through deflection of their hair bundles, an array of modified microvilli known as stereocilia, organized into rows of graduated heights forming a staircase pattern. The tip link, a fibrous link connecting the tip of each transducing stereocilium to the side of its taller neighbor, gates the mechanoelectrical transduction channel(s) located at the tip of the shorter stereocilium (Fig. 2*A*). Mutations of USH1 genes affect hair bundle morphogenesis and tip-link maintenance in the inner ear hair cells (5).

Adenoassociated virus (AAV)-mediated gene transfer has emerged as a promising strategy for treating hereditary diseases (6, 7). AAV vectors have different cell tropisms, and can mediate high levels of transgene expression. These properties have led to their use in preclinical and clinical trials for several inherited disorders, including genetic forms of Parkinson's disease, metabolic disorders, and retinal diseases, but they have not yet been used for inner ear diseases (6–10). Various viral vectors containing *GFP* as a reporter gene have been shown to transduce inner ear hair cells (11–15), and several studies have investigated the use of gene therapy to restore hearing and balance in animal models, with different degrees of success. However, to date, partial hearing improvement was only obtained for mouse models without severe dysmorphogenesis of the inner ear hair cells (16–22). Here, we focused on the genetic form of USH1 caused by mutations of *USH1G*, encoding the submembrane scaffold protein sans (23, 24). *Ush1g*$^{-/-}$ mutant mice display profound deafness and vestibular dysfunction, characterized by circling behavior and head

Significance

Hearing and balance impairments are major concerns and a serious burden for public health, but still lack an effective curative therapy. We assessed inner ear functions in a mouse model of Usher syndrome type 1, a developmental disorder characterized by profound congenital deafness and balance deficit, after local gene therapy. Viral transfer of the wild-type cDNA to the inner ear of the mutant mice shortly after birth resulted in a partial restoration of hearing and a long-lasting, almost complete, removal of the balance defect. The present results provide a basis for future clinical trials in humans.

Author contributions: C.P. and S.S. designed research; A.E., V.M., A.L., O.A., J.B.d.M., G.L., A.M., T.D., S.N., F.F.d.B., M.B., D.D., L.L., P.A., and S.S. performed research; C.P. and S.S. contributed new reagents/analytic tools; A.E., V.M., J.B.d.M., E.E., and S.S. analyzed data; and A.E., V.M., J.B.d.M., J.-P.H., C.P., and S.S. wrote the paper.

Reviewers: K.B.A., Tel Aviv University; and D.D., Université Pierre-et-Marie-Curie.

Conflict of interest statement: A patent involving A.E., C.P., and S.S. (PCT/EP2016/053613) has been deposited by the Institut Pasteur, INSERM, and CNRS.

Freely available online through the PNAS open access option.

[1]C.P. and S.S. contributed equally to this work.

[2]To whom correspondence may be addressed. Email: christine.petit@pasteur.fr or saaid.safieddine@pasteur.fr.

This article contains supporting information online at www.pnas.org/lookup/suppl/doi:10.1073/pnas.1708894114/-/DCSupplemental.

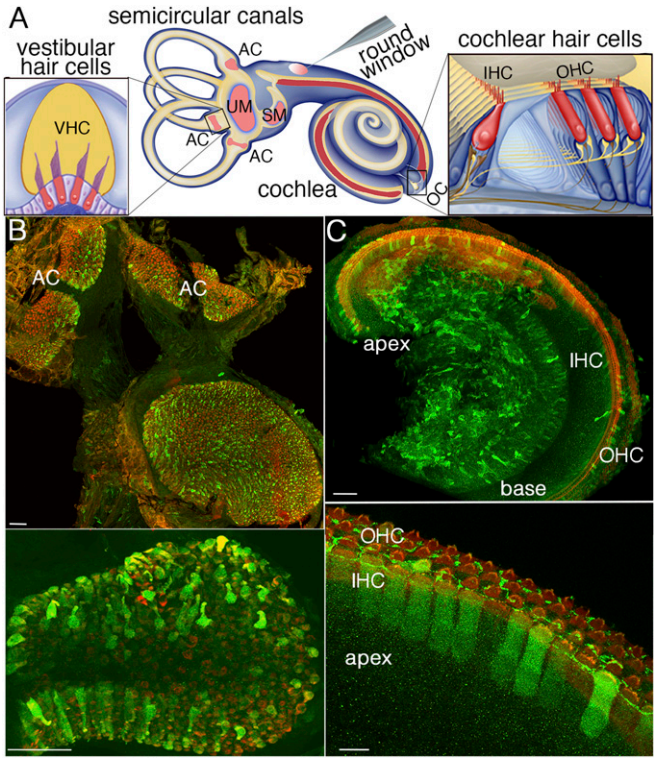

Fig. 1. AAV8 vector (Penn Vector Core) transduces vestibular and cochlear hair cells with different efficiencies. (*A*) Diagram of the mouse inner ear and viral injection through the round window of the cochlea. The vestibular sensory epithelia [AC, ampullar crista(e) of the three semicircular canals; SM, saccular macula; UM, utricular macula] and cochlear sensory epithelium (OC, organ of Corti) are drawn in pink and in red, respectively. Details of an AC and the OC are presented on the left side and right side of this diagram, respectively, with the hair cells (IHCs, OHCs, and VHCs) drawn in red. The AAV8-*Sans-IRES-GFP* (Penn Vector Core) recombinant virus injected through the cochlear round window of a mouse on P2.5 transduces the vast majority of VHCs (*B*, *Upper*) and transduces cochlear IHCs and OHCs more efficiently in the apical region than in the basal region of the cochlea (*C*, *Upper*), as shown by the GFP labeling (green) on P8.5. All hair cells are stained red by an anti-myosin VI antibody. Higher magnification views of the AC (*B*, *Lower*) and the OC (*C*, *Lower*) from the cochlear apical region are shown. (Scale bars: *Upper*, 50 μm; *Lower*, 10 μm.)

tossing. The hair bundles of their cochlear hair cells and vestibular hair cells (VHCs) undergo abnormal morphogenesis and lack functional tip links (24, 25). We explored the feasibility, reliability, and long-term efficacy of local gene therapy in these mice.

Results

Viral cDNA Transfer Restores Sans Expression and Targeting in Cochlear and VHCs of *Ush1g*$^{-/-}$ Mice. A number of AAV serotypes and over 100 naturally occurring AAV variants have been isolated from adenovirus stocks or from human/nonhuman primate tissues. They display different cell tropisms (14), but there are some discrepancies in their reported transduction efficiencies and cell tropisms in the inner ear (26–29). We thus investigated the ability of several AAV vectors to transduce the inner ear hair cells. We tested recombinant AAV1, AAV2, AAV5, and AAV8 vectors containing the green fluorescent protein (GFP) reporter gene driven by a hybrid promoter (CAG) consisting of the CMV enhancer fused to the chicken β-actin gene promoter. A single viral injection through the round window membrane separating the middle ear from the inner ear was performed in C57BL/6 wild-type mice on postnatal day 2.5 (P2.5) (Fig. 1*A*). The sensory epithelium of the cochlea (organ of Corti) and the vestibular end organs were microdissected on P8.5, and immunolabeled for otoferlin or myosin VI to visualize the inner ear hair cells, as well as for GFP. These recombinant AAV vectors transduced the inner ear cell types with different cell tropisms and transduction rates. In the cochlea, AAV1 (SignaGen) and AAV2 and AAV5 (Penn Vector Core) mostly transduced supporting cells of the organ of Corti, namely, Deiters' cells and inner phalangeal cells (Fig. S1 *A*–*C*). AAV8 from SignaGen (with the CAG promoter) mainly transduced cochlear ganglion neurons (Fig. S1*D*), whereas AAV8 from Penn Vector Core (with the same promoter) efficiently transduced hair cells and supporting cells (Fig. S1*E*). There are two types of cochlear hair cells: the inner hair cells (IHCs), which are the genuine auditory sensory cells that transmit the encoded sensory signal to the central nervous system, and the outer hair cells (OHCs), which function as fine-tuned amplifiers of the sound stimulus (30) (Fig. 1*A*). After injection of AAV8 from Penn Vector Core, more IHCs expressed GFP at the apex of the cochlea (84 ± 3%) than at the base (40% ± 0.5%), whereas OHCs were transduced with roughly the same efficiency at the base (28 ± 3%) and at the apex (24 ± 2%) (n = 23 mice; Fig. S1 *E* and *F*). Surgery and intracochlear injection of the virus did not affect auditory brainstem responses (ABRs) tested from 2 to 12 wk after injection (see Fig. 4*A* and Fig. S4; Mann–Whitney test, P = 0.7).

We then investigated the efficiency with which the recombinant AAV8-*Sans*-internal ribosome entry site (*IRES*)-*GFP* virus (Penn Vector Core) containing the murine cDNA *Sans*, encoding the unique spliced transcript of *Ush1g*, transduced inner ear hair cells. *Ush1g*$^{+/-}$ mice were injected with the recombinant virus on P2.5, and 6 d later, the sensory epithelia of the cochlea and vestibular end organs were microdissected and immunolabeled either for GFP and myosin VI or for GFP and sans. The hair cell transduction efficacy of AAV8-*Sans-IRES-GFP* was similar to that of AAV8-*GFP* (Fig. 1 *B* and *C*). The rate of IHC transduction (i.e., *GFP*-expressing IHCs) was 87 ± 4% at the cochlear apex, gradually decreasing to 45 ± 6% at the cochlear base, and the rate of OHC transduction was 33 ± 6% at the apex, gradually decreasing to 25 ± 5% at the base (n = 24 mice; Fig. 1*C*). Surprisingly, in the vestibular end organs of the injected ears, the hair cells were transduced at a much higher rate, 91 ± 24% (n = 17 mice; Fig. 1*B*). Moreover, the injection of AAV8-*Sans-IRES-GFP* into the cochlea of *Ush1g*$^{-/-}$ mice restored a normal targeting of the sans protein to the tips of the stereocilia of transduced IHCs, OHCs, and VHCs on P8.5 (24, 25) (Fig. 2).

Viral Transfer of the *Sans* cDNA to the Hair Cells Rescues *Ush1g*$^{-/-}$ Mice from Hair Bundle Defects. From embryonic day 17.5 (E17.5) onward, cochlear hair cells of *Ush1g*$^{-/-}$ mice display fragmented hair bundles with reduced numbers of stereocilia and mispositioned kinocilia (24, 25), and nearly all VHCs have collapsed hair bundles. The degeneration of the middle and short rows of stereocilia in IHCs and OHCs and the collapse of the VHC hair bundles are even more pronounced at P2.5 (Fig. 3*A* and Fig. S2). We investigated whether the viral expression of the *Sans* cDNA in the hair cells rescued the mice from these defects by scanning electron microscopy analysis. In the injected *Ush1g*$^{-/-}$ mice, the vast majority of hair bundles of IHCs, OHCs of the cochlear apex, and VHCs displayed a typical staircase pattern (81 ± 3% for cochlear hair cells, n = 72 cells and 70 ± 1% for VHCs, n = 304 cells from 10 mice). Notably, the stereocilia of the short and middle rows in most IHCs (93 ± 2%, n = 27 cells) and OHCs (68 ± 5%, n = 55 cells) in the apical region of the injected cochlea had prolate tips pointing toward their taller neighbors, just like in *Ush1g*$^{+/-}$ control mice. The stereocilia tips of most VHCs had their characteristic prolate shape too. Prolate tips are considered a hallmark of the presence of functional tip links resulting from the pulling force exerted by these links on the tips of the stereocilia (31). By contrast, the stereocilia tips had

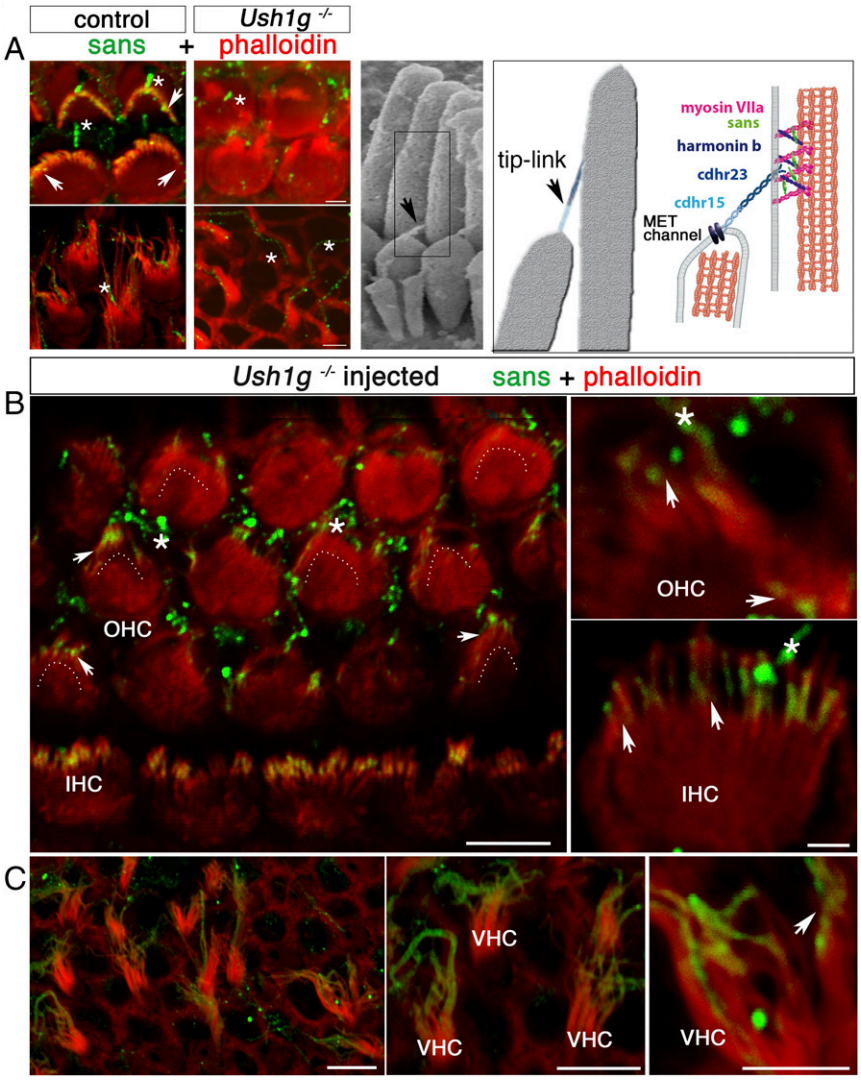

Fig. 2. AAV8-*Sans-IRES-GFP* restores sans expression and targeting in the inner ear hair cells of *Ush1g*$^{-/-}$ mice. (*A*, *Left*) OHC (*Upper*) and VHC (*Lower*) hair bundles from P8.5 wild-type (control) and *Ush1g*$^{-/-}$ mice, immunostained for sans (green) and stained for F-actin with phalloidin (red). Sans is detected at the tips of the stereocilia in the wild-type mouse (white arrowheads), but not in the *Ush1g*$^{-/-}$ mouse. A nonspecific staining of the kinocilium is present both in the wild-type and *Ush1g*$^{-/-}$ mice (asterisks). (*A*, *Center*) Scanning electron micrograph of the IHC hair bundle, showing the tip links between adjacent stereocilia of different rows (black arrowhead). (*A*, *Right*) Diagram showing the tip-link lower and upper insertion points, the position of the mechanoelectrical transduction (MET) channel(s) at the tip of the shorter stereocilium, and the locations of the five USH1 proteins forming the tip link [cadherin-related proteins 15 (cdhr15) and 23 (cdhr23)] or presumably involved in its anchoring to the actin filaments of the taller stereocilium (harmonin b, sans, and myosin VIIa). The submembrane scaffold protein sans belongs to the tip-link upper insertion point molecular complex. Top views of the organ of Corti in the cochlear apical region (*B*) and of the utricular macula (*C*) of an injected *Ush1g*$^{-/-}$ mouse on P8.5 and high-magnification photographs of OHC, IHC, and VHC hair bundles are shown. Sans is targeted to the tips of the stereocilia in all hair cell types (arrowheads). The image in *B* is extracted from a larger tile scan and contains two tiles stitched together at the upper part of the image. Dashed lines in *B* indicate the position of the hair bundle base (V shape) in OHCs expressing the transgene. (Scale bars: 5 μm.)

prolate shapes in only 4% of the VHCs (n = 204 cells) and none of the cochlear hair cells (n = 147 cells, from seven mice) of uninjected *Ush1g*$^{-/-}$ mice (Fig. 3*A*, *Insets*; Mann–Whitney test, $P < 10^{-4}$ for all comparisons between injected and uninjected *Ush1g*$^{-/-}$ mice), which is consistent with the loss of tip links in these mice (24). Finally, we estimated the numbers of stereocilia per hair bundle, their projected heights, and their spacing, based on our scanning electron micrographs (Table S1). We found no significant differences in any of these parameters between the injected *Ush1g*$^{-/-}$ mice and *Ush1g*$^{+/-}$ mice (Table S1). Of note, the cochlear and vestibular hair bundles of injected and uninjected wild-type mice did not differ in appearance either, suggesting that the injection through the round window membrane did not impair the morphological development of the hair bundles.

In keeping with the morphological rescue of the hair bundles, the transduced IHCs and OHCs of injected *Ush1g*$^{-/-}$ P8.5 mice, identified on the basis of GFP fluorescence, displayed mechanoelectrical transduction currents of much higher peak amplitudes (424 ± 69.4 pA in IHCs, n = 11 and 641 ± 35 pA in OHCs, n = 12) than IHCs and OHCs of uninjected *Ush1g*$^{-/-}$ mice (110.8 ± 30.8 pA in IHCs, n = 5 and 47.3 ± 5.7 pA in OHCs, n = 4; Student's t test, $P < 0.01$ for each comparison; Fig. 3*B*). In addition, the sensitivity of the transduction current response to hair bundle displacement was similar in injected *Ush1g*$^{-/-}$ mice and injected *Ush1g*$^{+/-}$ (control) mice (calculated mean sensitivity values: 1.12 ± 0.19 μm^{-1} and 1.30 ± 0.14 μm^{-1} for IHCs, and 1.73 ± 0.2 μm^{-1} and 2.24 ± 0.15 μm^{-1} for OHCs of injected *Ush1g*$^{+/-}$ and injected *Ush1g*$^{-/-}$ mice, respectively; unpaired t test, $P > 0.1$ for both comparisons) (24) (Fig. 3*B* and Fig. S3*A*).

Partial Restoration of Hearing. *Ush1g*$^{-/-}$ mice are profoundly deaf and show no identifiable ABRs, even in response to sounds of intensities up to 110 dB sound pressure level (SPL) (24) (Fig. 4*A*). After gene transfer, ABR waves could be recorded in 2- to 12-wk-old *Ush1g*$^{-/-}$ mice for sound intensities exceeding 75 dB SPL, indicating a substantial improvement in cochlear function. For sounds in the low-frequency range (5–15 kHz), the hearing threshold elevation was about 50 dB on P30, instead of a complete hearing loss in the uninjected mutant mice (n = 18 injected mice; one-way ANOVA test, $P < 0.01$; Fig. 4*A*). The improvement of hearing thresholds was less noticeable at higher frequencies (20–40 kHz), which is consistent with the decrease in cochlear hair cell transduction rates from the apical region to the basal region of the cochlea, where high-frequency tones are analyzed (32) (Fig. S1*F*). It is noteworthy that a partial hearing rescue was still present at the age of 12 wk, the oldest age at which the mice were tested (33) (Fig. S4). Thus, a single intracochlear injection of the transgene during the neonatal period

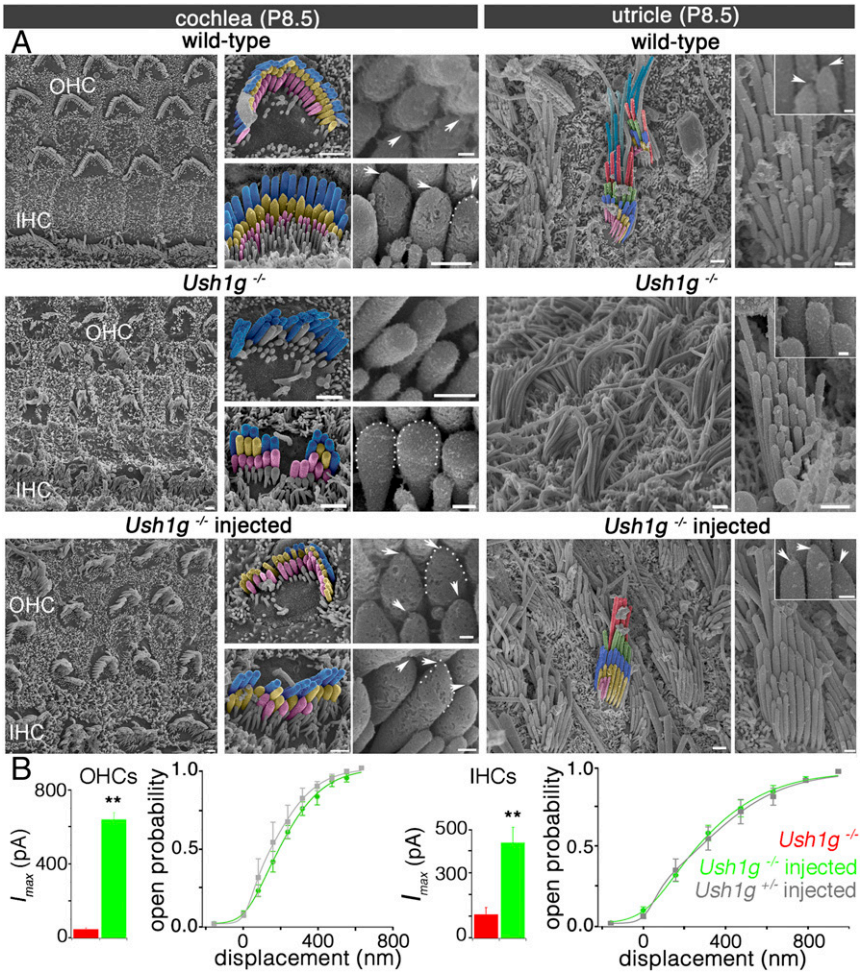

Fig. 3. *Sans* cDNA transfer to inner ear hair cells rescues *Ush1g*$^{-/-}$ mice from hair bundle structural defects. (*A*) Low-, intermediate-, and high-magnification scanning electron micrographs showing the architecture of the hair bundles in cochlear OHCs and IHCs (*Left*) and in VHCs (utricle, *Right*) of a control wild-type mouse, an *Ush1g*$^{-/-}$ mouse, and an *Ush1g*$^{-/-}$ mouse injected with the *Sans* cDNA, on P8.5. In the wild-type mouse, the stereocilia tips have prolate shapes, which is the hallmark of functional tip links (arrowheads and dashed lines) (31), whereas they have rounded shapes in the *Ush1g*$^{-/-}$ mouse (dashed lines), in keeping with the loss of the tip links (24). Note the fragmentation of the hair bundles and the degeneration of some stereocilia in this mouse. In the injected *Ush1g*$^{-/-}$ mouse, the hair bundles have recovered their normal staircase architecture and the prolate shapes of stereocilia tips (arrowheads and dashed line). (Scale bars: 2 μm.) (*B*) Mechanoelectrical transduction (MET) currents recorded ex vivo in IHCs and OHCs of uninjected *Ush1g*$^{-/-}$ (red), injected *Ush1g*$^{-/-}$ (green), and injected *Ush1g*$^{+/-}$ (control, gray) P8.5 mice. Bar charts show the peak amplitudes of the MET currents (I_{max}) recorded in the hair cells of uninjected or injected *Ush1g*$^{-/-}$ mice (110.8 ± 30.8 pA in IHCs and 47.3 ± 5.7 pA in OHCs of uninjected *Ush1g*$^{-/-}$ mice vs. 424 ± 70 pA in IHCs and 641 ± 35 pA in OHCs of injected *Ush1g*$^{-/-}$ mice). Note the marked increase of I_{max} in the injected *Ush1g*$^{-/-}$ mice compared with the noninjected mice (Student's *t* test, $^{**}P < 0.01$ for both IHCs and OHCs*)*. Line graphs show the MET channel opening probability plotted as a function of hair bundle displacement for IHCs and OHCs of injected *Ush1g*$^{+/-}$ (gray) and *Ush1g*$^{-/-}$ (green) mice. For both cell types, the two curves are superimposed.

was able to restore the hearing of loud sounds (≥75 dB) of low frequency in *Ush1g*$^{-/-}$ mice.

Complete Restoration of Vestibular Function. Video-tracking in an open-field chamber showed that injected *Ush1g*$^{-/-}$ mice explored the field in a manner similar to control mice, without circling behavior (1.5 ± 0.4 turn in 2 min for injected *Ush1g*$^{-/-}$ mice, $n = 10$, vs. 20.3 ± 2.8 turns in 2 min for uninjected *Ush1g*$^{-/-}$ mice, $n = 7$; Student's *t* test, $P < 0.01$; Fig. 4*B*, Fig. S3*B*, and Movies S1–S4). Additional behavioral tests were carried out to assess the vestibular functions in these mice, up to 53 wk after injection (31). In the balance platform test (*SI Materials and Methods*), the uninjected *Ush1g*$^{-/-}$ mice ($n = 7$) were unable to stay on the platform, whereas the injected *Ush1g*$^{-/-}$ mice ($n = 10$), like the *Ush1g*$^{+/-}$ control mice ($n = 9$), were able to spend about 1 min on the platform (58.4 ± 0.9 s vs. 27.6 ± 10.6 s for injected *Ush1g*$^{-/-}$ mice and uninjected mutant mice, respectively; Student's *t* test, $P < 0.01$). Likewise, the injected *Ush1g*$^{-/-}$ mice responded normally in the trunk curl test, and were able to reach a horizontal landing surface rapidly when suspended by the tail, without curling the trunk toward their tail, whereas the uninjected mutant mice were unable to land on the horizontal surface, instead curling toward the base of the tail when suspended (Pearson's χ^2 test, $P < 0.01$). In a contact righting test, the injected *Ush1g*$^{-/-}$ mice could reorient their bodies rapidly upon inversion of the tube in which they were held, whereas the uninjected *Ush1g*$^{-/-}$ mice could not (Pearson's χ^2 test, $P < 0.01$). In the swim test described by Hardisty-Hughes et al. (34), the injected *Ush1g*$^{-/-}$ mice behaved just like the wild-type mice, whereas the uninjected *Ush1g*$^{-/-}$ mice displayed underwater tumbling, and had to be lifted out and rescued at once (Pearson's χ^2 test, $P < 0.01$). These results suggest that gene replacement therapy by early postnatal injection of AAV8-*Sans* into the inner ear restores the vestibular function in *Ush1g*$^{-/-}$ mice. Notably, this effect persisted in the long term, as no difference was found between the *Ush1g*$^{+/-}$ and injected *Ush1g*$^{-/-}$ mice when these tests were carried out 53 wk after treatment (platform test: Student's *t* test, $P > 0.1$; swim

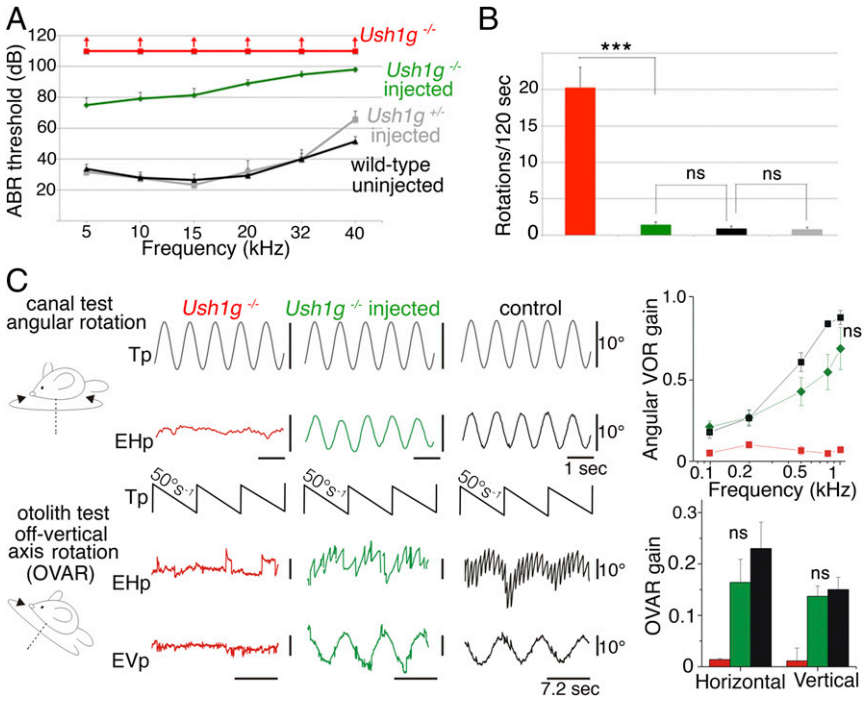

Fig. 4. *Sans* cDNA transfer improves hearing thresholds of injected *Ush1g*$^{-/-}$ mice and almost completely restores their vestibular functions. (*A*) ABR thresholds in P30 wild-type mice (not injected) and P30 *Ush1g*$^{+/-}$ and *Ush1g*$^{-/-}$ mice injected or not injected with AAV8-*Sans-IRES-GFP* on P2.5. ABRs were recorded in response to 5- to 40-kHz tone bursts, and for sound intensities between 10 and 110 dB SPL. The ABR threshold elevation is about 50 dB for low-frequency sounds (5–15 kHz) in injected *Ush1g*$^{-/-}$ mice ($n = 18$ mice), instead of a complete hearing loss in the uninjected mutant mice ($n = 3$ mice). Note that the viral injection did not affect the ABR thresholds of *Ush1g*$^{+/-}$ heterozygous mice ($n = 7$), compared with the uninjected wild-type (control) mice ($n = 6$). (*B*) Bar chart showing the number of rotations in open-field recordings of mouse displacements over a period of 2 min (120 s) in 33-wk-old *Ush1g*$^{+/-}$ (control) and *Ush1g*$^{-/-}$ mice injected or not injected with the transgene on P2.5. ***$P < 0.001$. (*C*) Vestibulo-ocular recordings done between 10 and 12 mo after injection of the transgene. (*Upper*) Semicircular canal test. An angular VOR (aVOR) was recorded during horizontal sinusoidal rotations of the turntable (the representation of the table signal, Tp, is inverted for easy comparison). No aVOR is detected in the uninjected *Ush1g*$^{-/-}$ mouse (EHp, red trace), whereas the injected *Ush1g*$^{-/-}$ mouse (green trace) displays an aVOR response similar to that of the control mouse (black trace). The line graph shows the responses for stimuli of different speeds (from 0.1 to 1 Hz) (mean ± SEM, $n = 5$ mice in each group; ANOVA, $P = 0.2$). (*Lower*) Otolithic organ test using off-vertical axis rotation (OVAR). No eye response is detected in the *Ush1g*$^{-/-}$ mouse (EHp and EVp, red traces), whereas the injected *Ush1g*$^{-/-}$ mouse (green traces) and the control mouse (black traces) display compensatory eye movements. The bar chart shows the horizontal and vertical responses (mean ± SEM, $n = 5$ mice in each group; Mann–Whitney test, $P = 0.3$ and $P = 0.5$ for the comparison of the horizontal and vertical responses between the control and injected *Ush1g*$^{-/-}$ mice, respectively). EHp, eye horizontal position (eye movements to the right are represented upward); EVp, eye vertical position; ns, statistically not significant; Tp, table position.

test: Pearson's χ^2 test, $P > 0.1$; $n = 5$ mice for each genotype). We then evaluated the long-term contributions of the different vestibular end organs to the improvement in equilibration up to 67 wk. The functions of the semicircular canals and otolith organs (saccule and utricle) were assessed by recording vestibulo-ocular reflexes (VORs) and macula-ocular reflexes (MORs) in response to specific turntable movements, respectively (35). No compensatory eye movements in response to turntable rotation could be detected in *Ush1g*$^{-/-}$ mice, indicating a complete loss of function for both the semicircular canals and otolith organs, as expected. By contrast, all of the injected *Ush1g*$^{-/-}$ mice showed compensatory eye movements in the VOR and MOR tests (Fig. 4*C*). Vestibulo-ocular responses were indistinguishable from those of wild-type mice in two of the five injected mice. In the other three mice, semicircular canal organ responses were restored to a lesser degree than otolith organ responses, which were not significantly different from those of controls, demonstrating that a single intracochlear injection of the transgene results in a long-lasting complete restoration of the vestibular function in *Ush1g*$^{-/-}$ mice.

Discussion

We demonstrate a long-term restoration of inner ear functions in a mouse model of USH1 by using a single AAV-mediated local gene therapy at an early postnatal stage. The recombinant AAV8, with the CAG promoter driving transgene expression, was found to be the most efficient of the AAV vectors tested for the transduction of inner ear hair cells. Virus injection through the round window membrane on P2.5 had no deleterious effect on inner ear development in wild-type mice. Furthermore, no adverse side effects were detected in the mice for up to 63 wk after virus injection. This approach therefore appears as a promising one to attempt in future extension to human patients.

Our results demonstrate that *Sans* cDNA delivery restores the production and localization of the sans protein in the IHCs, OHCs, and VHCs, suggesting that the exogenous protein was correctly targeted to the tip-link insertion points (24, 36) (Fig. 2). Moreover, the transduced cochlear hair cells of injected *Ush1g*$^{-/-}$ mice displayed markedly improved mechanoelectrical transduction currents in ex vivo experiments on P8.5 cochlear explants, which indicates that expression of the *Sans* cDNA in these cells effectively compensates for the absence of the native protein. From these results, we can infer that the exogenous protein most probably interacts with the other members of the USH1 protein complex (i.e., cadherin-related protein 23, cadherin-related protein 15, myosin VIIA, harmonin), as required for the correct functioning of the mechanoelectrical transduction channels (24) (Fig. 2*A*). Transduction currents can first be recorded on P0 and P2 in the hair cells of the cochlear basal and apical regions, respectively (37),

whereas the transduction apparatus of VHCs is already functional on E17 (37, 38). In this study, the *Sans* cDNA was delivered by a viral vector on P2.5, and expression of the cDNA was first detected 48 h later (i.e., about 10 d after the normal onset of *Ush1g* expression on E14.5). Despite this delay, gene replacement therapy efficiently restored the structure and function of inner ear hair cells in *Ush1g*$^{-/-}$ mice and prevented the balance deficit while limiting the hearing impairment for low sound frequencies. The time window for treating deafness and balance disorders by gene transfer in patients with USH1 may therefore be larger than initially thought. In addition, the almost complete restoration of vestibular functions reported here reveals unanticipated temporal flexibility for the effective treatment of other early-onset balance disorders of genetic origin. Further studies are required to determine why the transgene injection did not fully restore cochlear function in *Ush1g*$^{-/-}$ mice. The higher rates of hair cell transduction in the vestibular end organs than in the cochlea raise the hope of a full restoration of hearing by increasing the transduction rates in the cochlear hair cells (22). It is worthy of note that hearing thresholds were significantly improved for sounds in the low-frequency range (5–15 kHz), which are analyzed in a cochlear apical region that, owing to its high curvature, cannot be reached by the electrode arrays of cochlear implants (39). Therefore, this gene therapy approach might be effective in association with current cochlear implants by partly restoring the tonotopic information that these implants cannot provide, and thus allowing for better sound perception.

This study constitutes a significant step toward the virus-mediated cure of a form of genetic deafness in humans. However, before considering translation to clinical trials, these results must be reproduced in larger animal models that are better predictors of responses in humans than rodents, based on the size and the kinetics of maturation of their cochlea.

Materials and Methods

Detailed information is provided in *SI Materials and Methods*. Animal experiments were carried out in accordance with INSERM and Institut Pasteur welfare guidelines. Animals were housed in the Institut Pasteur animal facilities accredited by the French Ministry of Agriculture for experiments on live mice. The intracochlear viral injection procedure, approved by the Animal Care and Use Committee of the Institut Pasteur, was carried out as described by Akil et al. (16). Immunofluorescence analyses were carried out as described elsewhere (40, 41). Scanning electron microscopy analysis was done as described elsewhere (24). Electrophysiological whole-cell patch-clamp recordings of hair cell mechanoelectrical transduction currents were carried out in cochlear explants from P8.5 mice, as described by Michalski et al. (42). ABRs to sound stimuli were recorded and analyzed as previously described (43). The various tests to assess vestibular function were carried out as previously reported (34, 35).

ACKNOWLEDGMENTS. We thank Jean-Marc Panaud (Reprography Service, Institut Pasteur) for assistance with SEM image colorization. This work was supported by Fondation pour la Recherche Médicale (A.E.); the European Union Seventh Framework Programme under the grant agreement HEALTH-F2-2010-242013 (TREATRUSH); the European Commission (ERC-2011-ADG_294570); French state funds managed by Agence Nationale de la Recherche within the Investissements d'Avenir Programme (ANR-15-RHUS-0001); LabEx Lifesenses (ANR-10-LABX-65); and grants from the BNP Paribas Foundation, the FAUN-Stiftung, the LHW-Stiftung, and Errera Hoechstetter.

1. Jeon EK, Turner CW, Karsten SA, Henry BA, Gantz BJ (2015) Cochlear implant users' spectral ripple resolution. *J Acoust Soc Am* 138:2350–2358.
2. Vivero RJ, Fan K, Angeli S, Balkany TJ, Liu XZ (2010) Cochlear implantation in common forms of genetic deafness. *Int J Pediatr Otorhinolaryngol* 74:1107–1112.
3. Friedman TB, Schultz JM, Ahmed ZM (2005) Usher syndrome type 1: Genotype-phenotype relationships. *Retina* 25(Suppl):S40–S42.
4. Liu XZ, et al. (2008) Cochlear implantation in individuals with Usher type 1 syndrome. *Int J Pediatr Otorhinolaryngol* 72:841–847.
5. Petit C, Richardson GP (2009) Linking genes underlying deafness to hair-bundle development and function. *Nat Neurosci* 12:703–710.
6. Collins M, Thrasher A (2015) Gene therapy: Progress and predictions. *Proc Biol Sci* 282: 20143003.
7. Simonato M, et al. (2013) Progress in gene therapy for neurological disorders. *Nat Rev Neurol* 9:277–291.
8. Asokan A, Schaffer DV, Samulski RJ (2012) The AAV vector toolkit: Poised at the clinical crossroads. *Mol Ther* 20:699–708.
9. Kotterman MA, Schaffer DV (2014) Engineering adeno-associated viruses for clinical gene therapy. *Nat Rev Genet* 15:445–451.
10. Mingozzi F, High KA (2011) Therapeutic in vivo gene transfer for genetic disease using AAV: Progress and challenges. *Nat Rev Genet* 12:341–355.
11. Iizuka T, et al. (2008) Noninvasive in vivo delivery of transgene via adeno-associated virus into supporting cells of the neonatal mouse cochlea. *Hum Gene Ther* 19: 384–390.
12. Kilpatrick LA, et al. (2011) Adeno-associated virus-mediated gene delivery into the scala media of the normal and deafened adult mouse ear. *Gene Ther* 18:569–578.
13. Konishi M, Kawamoto K, Izumikawa M, Kuriyama H, Yamashita T (2008) Gene transfer into guinea pig cochlea using adeno-associated virus vectors. *J Gene Med* 10: 610–618.
14. Wu Z, Asokan A, Samulski RJ (2006) Adeno-associated virus serotypes: Vector toolkit for human gene therapy. *Mol Ther* 14:316–327.
15. Xia L, Yin S, Wang J (2012) Inner ear gene transfection in neonatal mice using adeno-associated viral vector: A comparison of two approaches. *PLoS One* 7:e43218.
16. Akil O, et al. (2012) Restoration of hearing in the VGLUT3 knockout mouse using virally mediated gene therapy. *Neuron* 75:283–293.
17. Askew C, et al. (2015) Tmc gene therapy restores auditory function in deaf mice. *Sci Transl Med* 7:295ra108.
18. Chang Q, et al. (2015) Virally mediated Kcnq1 gene replacement therapy in the immature scala media restores hearing in a mouse model of human Jervell and Lange-Nielsen deafness syndrome. *EMBO Mol Med* 7:1077–1086.
19. Chien WW, et al. (2016) Gene therapy restores hair cell stereocilia morphology in inner ears of deaf whirler mice. *Mol Ther* 24:17–25.
20. Isgrig K, et al. (2017) Gene therapy restores balance and auditory functions in a mouse model of Usher syndrome. *Mol Ther* 25:780–791.
21. Landegger LD, et al. (2017) A synthetic AAV vector enables safe and efficient gene transfer to the mammalian inner ear. *Nat Biotechnol* 35:280–284.
22. Pan B, et al. (2017) Gene therapy restores auditory and vestibular function in a mouse model of Usher syndrome type 1c. *Nat Biotechnol* 35:264–272.
23. Weil D, et al. (2003) Usher syndrome type I G (USH1G) is caused by mutations in the gene encoding SANS, a protein that associates with the USH1C protein, harmonin. *Hum Mol Genet* 12:463–471.
24. Caberlotto E, et al. (2011) Usher type 1G protein sans is a critical component of the tip-link complex, a structure controlling actin polymerization in stereocilia. *Proc Natl Acad Sci USA* 108:5825–5830.
25. Lefèvre G, et al. (2008) A core cochlear phenotype in USH1 mouse mutants implicates fibrous links of the hair bundle in its cohesion, orientation and differential growth. *Development* 135:1427–1437.
26. Derby ML, Sena-Esteves M, Breakefield XO, Corey DP (1999) Gene transfer into the mammalian inner ear using HSV-1 and vaccinia virus vectors. *Hear Res* 134:1–8.
27. Raphael Y, Frisancho JC, Roessler BJ (1996) Adenoviral-mediated gene transfer into guinea pig cochlear cells in vivo. *Neurosci Lett* 207:137–141.
28. Sacheli R, Delacroix L, Vandenackerveken P, Nguyen L, Malgrange B (2013) Gene transfer in inner ear cells: A challenging race. *Gene Ther* 20:237–247.
29. Wang Y, et al. (2013) Early postnatal virus inoculation into the scala media achieved extensive expression of exogenous green fluorescent protein in the inner ear and preserved auditory brainstem response thresholds. *J Gene Med* 15:123–133.
30. Fettiplace R, Hackney CM (2006) The sensory and motor roles of auditory hair cells. *Nat Rev Neurosci* 7:19–29.
31. Prost J, Barbetta C, Joanny JF (2007) Dynamical control of the shape and size of stereocilia and microvilli. *Biophys J* 93:1124–1133.
32. Kandler K, Clause A, Noh J (2009) Tonotopic reorganization of developing auditory brainstem circuits. *Nat Neurosci* 12:711–717.
33. Johnson KR, Erway LC, Cook SA, Willott JF, Zheng QY (1997) A major gene affecting age-related hearing loss in C57BL/6J mice. *Hear Res* 114:83–92.
34. Hardisty-Hughes RE, Parker A, Brown SD (2010) A hearing and vestibular phenotyping pipeline to identify mouse mutants with hearing impairment. *Nat Protoc* 5:177–190.
35. Romand R, et al. (2013) Retinoic acid deficiency impairs the vestibular function. *J Neurosci* 33:5856–5866.
36. Grati M, Kachar B (2011) Myosin VIIa and sans localization at stereocilia upper tip-link density implicates these Usher syndrome proteins in mechanotransduction. *Proc Natl Acad Sci USA* 108:11476–11481.
37. Géléoc GS, Holt JR (2014) Sound strategies for hearing restoration. *Science* 344: 1241062.
38. Denman-Johnson K, Forge A (1999) Establishment of hair bundle polarity and orientation in the developing vestibular system of the mouse. *J Neurocytol* 28:821–835.
39. Van Abel KM, et al. (2015) Hearing preservation among patients undergoing cochlear implantation. *Otol Neurotol* 36:416–421.
40. Roux I, et al. (2009) Myosin VI is required for the proper maturation and function of inner hair cell ribbon synapses. *Hum Mol Genet* 18:4615–4628.
41. Roux I, et al. (2006) Otoferlin, defective in a human deafness form, is essential for exocytosis at the auditory ribbon synapse. *Cell* 127:277–289.
42. Michalski N, et al. (2009) Harmonin-b, an actin-binding scaffold protein, is involved in the adaptation of mechanoelectrical transduction by sensory hair cells. *Pflugers Arch* 459:115–130.
43. Delmaghani S, et al. (2015) Hypervulnerability to sound exposure through impaired adaptive proliferation of peroxisomes. *Cell* 163:894–906.